

0.9 T static magnetic field and temperature-controlled specimen environment for use with general-purpose optical microscopes

T. A. Harroun

National Research Council, Chalk River Laboratories, Chalk River, Ontario K0J 1J0, Canada
and Department of Physics, University of Guelph, Guelph, Ontario N1G 2W1, Canada

C. M. Desrochers, M.-P. Nieh, and M. J. Watson

National Research Council, Chalk River Laboratories, Chalk River, Ontario K0J 1J0, Canada

J. Katsaras

National Research Council, Chalk River Laboratories, Chalk River, Ontario K0J 1J0, Canada
Biophysics Interdepartmental Group and Guelph-Waterloo Institute of Physics, University of Guelph, Guelph, Ontario, Canada

(Received 13 October 2005; accepted 27 November 2005; published online 18 January 2006)

We describe the addition of a simple, low-cost 0.9 T fixed magnetic field to a commercially available, variable-temperature sample environment suitable for optical microscopy. The magnetic field is achieved with the use of Fe–Nd–B rare-earth permanent magnets and steel yoke assembly, packaged into a Linkam Scientific Instruments model THMS600 heating and cooling stage. We demonstrate its effectiveness with examples of magnetic ordering of a lipid/water system doped with paramagnetic Tm^{3+} ions in the presence and absence of the applied magnetic field and at different temperatures. © 2006 American Institute of Physics. [DOI: [10.1063/1.2162433](https://doi.org/10.1063/1.2162433)]

I. INTRODUCTION

A static magnetic field is an important specimen environment for many types of experimentation.^{1–3} For optical microscopy, there are many applications of a magnetic field such as observation of magnetic domains, examination of magnetotactic microorganisms, or the study of magnetic ordering of polymers and liquid crystals.^{4–7}

There are a number of challenges incorporating a strong magnetic field onto a specimen while under microscopic observation. One solution is to build the magnet and microscope around the unique requirements of the specimen. For example, Gmitrov *et al.*⁸ described a system for *in vivo* observation of a rabbit's ear blood circulation while under the influence of a magnetic field. Another method is to build the microscope inside the magnet. A notable example is given by Valles, Jr. *et al.*,⁹ who modified a Leica Monozoom 7 microscope to fit into the 195 mm bore of a resistive magnet located at the National High Magnetic Field Laboratory (Tallahassee, FL), and capable of exerting magnetic fields up to 16 T. For obvious reasons, all of the stock microscope's ferrous components had to be replaced with nonmagnetic equivalents.

The descriptions of incorporating magnetic-field capabilities to existing, general-purpose microscopes are less common. Modern benchtop research microscopes are highly modular instruments and can easily accommodate numerous microscopy techniques such as polarization, fluorescence, bright and dark fields, and numerous contrast enhancements. Furthermore, a number of after-market products that can easily be incorporated, such as micromanipulation, microinjection, electrical recording, and temperature control, are available. It is worthwhile, then, to provide an economical means

of integrating a magnetic field to a standard microscope, while maintaining access to all of its capabilities.

Only a few examples of adding magnetic capability to a general-purpose microscope can be found in the literature. Williams¹⁰ described an electromagnet, capable of more than 1 T, built to surround a microscope's objective. A Hall probe mounted near the sample monitors the field strength, which runs horizontally across the surface of a standard microscope slide. Oldenbourg and Phillips¹¹ illustrated an Fe–Nd–B permanent magnet assembly capable of exerting a magnetic field of more than 2 T, which is very uniform across 2 mm. The magnetic-field strength is varied by changing the gap between the steel pole pieces, which runs parallel to the sample capillary tube running lengthwise through the magnets. Although these approaches have the capabilities of altering the strength of the applied magnetic field, Cugat *et al.*¹² have constructed a variable flux system, which can change the field direction and add the possibility of a gradient. This system is based on combining the fields of several rotating rod magnets, magnetized in their radial direction. Although the maximum field strength at the sample is less than 0.04 T, it is very homogenous across a comparatively wide dimension of 7 mm. Although each of these approaches adds magnetic capability to a microscope, they are very bulky, and more importantly, are not thermostated.

This note describes our design of an economical, static field magnet system incorporated into a popular and commercially available heating/cooling microscope stage. The Linkam THMS600 (Surrey, UK) stage has a temperature range of -196 to 600 °C, with a programmable heating and cooling rate and temperature stability of better than 0.1 °C. Our design uses a 1018 cold-rolled steel yoke with

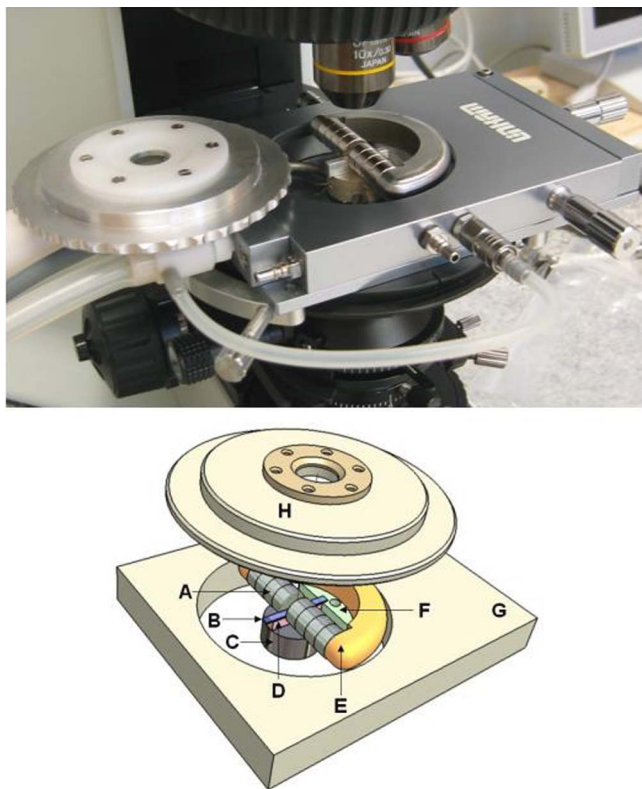


FIG. 1. (Color online) Photograph of the magnet assembly in the Linkam THMS600 heating/cooling microscope stage, mounted on an Olympus BX52 microscope (top). Schematic of the magnet assembly (bottom). The various parts are as follows: (A) eight 10-mm-diam and 5-mm-thick N42 Fe–Nd–B rare-earth permanent magnets with a 2 mm magnet gap. (B) Flat capillary sample container. (C) Heating/cooling block making good thermal contact with the aluminum interface spacer (D) used to place the sample at the center of the magnetic field. (E) 1018 steel yoke and (F) PTFE isolation block. (G) The body of the THMS600 temperature-controlled microscope stage and (H) associated cover.

Nd–Fe–B permanent magnets, producing a 0.9 T field in the middle of the sample. The magnet assembly fits neatly into the Linkam stage (Fig. 1). The absence of magnetic materials in the Linkam construction makes it an ideal base for this project. The only significant modification to the stage is a custom-built lid to accommodate the height of the magnet. We present some results of magnetic alignment of a liquid-crystal dispersion of phospholipids doped with TmCl₃ salt.

II. CONSTRUCTION DETAILS

Because of size constraints imposed by the THMS600 stage, we were effectively limited to the use of permanent magnets in constructing the magnet assembly. The important properties of permanent magnets are the residual induction, which determines the field strength of the magnet; the coercive force, which is the applied field strength required to reverse the magnetization; and the maximum-energy product, which is a measure of the available energy. Rare-earth and ceramic permanent magnets can have a residual induction up to 1.4 T, and can be fashioned into many different shapes. Fe–Nd–B magnets typically have the lowest cost compared to Sm–Co or Al–Ni–Co. However, care must be taken on the manufacturing grade of magnet, since the strongest and most common grades have maximum working tem-

perature of about 80 °C. Sintered N28EH-grade Fe–Nd–B has a higher working temperature of 120 °C at 1 T, but does not approach the 550 °C of grade-9 Al–Ni–Co. The coercive force of Al–Ni–Co magnets, however, is very low compared with Fe–Nd–B.

The top panel of Fig. 1 shows a picture of the magnet installed in the Linkam stage mounted on an Olympus BX52 microscope. The bottom panel shows a schematic in which we identify the various components that make up the temperature-regulated magnet assembly. In the present setup, eight 10-mm-diam and 5-mm-thick N42 Fe–Nd–B magnets (A) were used, separated by a 2 mm gap. This necessarily raises the height of the assembly to clear the stage's heating/cooling block (C), so the yoke (E) is affixed to a block of polytetrafluoroethylene (PTFE) (F).

The normal operation of the stage, without the magnet, includes an *x/y* sample manipulator, and a clip that helps the manipulator slide up over the heating/cooling block. In order to make sufficient space for the magnet assembly, these items are removed. The clip's screw hole in the stage body is then used to fasten the PTFE block.

An aluminium spacer [Fig. 1(D)] is used to place the capillary (B) containing the sample at the center of the magnetic field, and maintain good thermal conduct with the heating block. At this point, the magnet assembly protrudes above the THMS600 stage body, so a new lid was constructed to accommodate the new height, and is shown set off to the side in Fig. 1 (top panel). The lid was constructed in two pieces of PTFE and Al, with a thin quartz window and O-ring seal.

Raising the sample height has two important consequences regarding the microscope's operation, namely, that the original Linkam stage was designed to specific values of the working distances of the condenser and objective lenses. On the topside, the Linkam stage has a minimum working distance of about 4.5 mm with the standard lid in place, meaning that a 10× objective is the typical maximum magnification. Our new lid is built with the same working distance.

On the other side of the stage, Linkam provides a condenser extension lens with a longer working distance, since the sample is further from the condenser due to the thickness of the THMS600 body. Our design is such that we are at the limit of this 12.5 mm working distance, since the aluminum spacer block has raised the sample even further. In order to focus the condenser we had to remove the thin glass window on the underside of the THMS600, and the condenser lens now protrudes just inside the body. This, however, defeats the airtight sealed chamber necessary for precise control at extreme temperatures. A new condenser lens, with a slightly longer focal length, is required to restore 100% functionality.

The field was measured in 0.25 mm incremental steps with a Gauss meter (Lakeshore 410, Westervill, OH) having a square transverse-oriented Hall probe and a measuring area of 1 mm². Figure 2 shows the field strength between the permanent magnets and across the microscope's light path. The field varies from 9.4 kG near one of the quartet of magnets to 9.2 kG in the center. The width of the face of the permanent magnet is larger than the hole in which the mi-

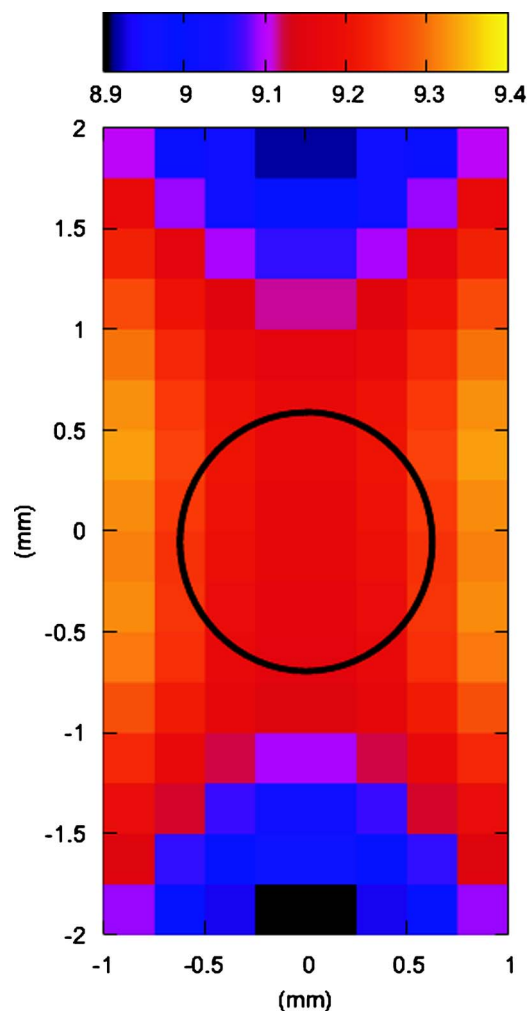


FIG. 2. (Color online) Two-dimensional map of the magnetic flux at the sample. The solid lines show the profile of the permanent magnets, and the circle is the light hole in the heating/cooling block. Midway between the magnets we measure a flux of ~ 0.9 T.

roscope's light passes through, providing for a nearly homogeneous field across the field of view. For polarization microscopy this is important, since it avoids the Faraday effect that would cause uneven rotation of the polarized light, and would not be canceled evenly by the polarization analyzer.

III. SYSTEM USED TO TEST THE MAGNET

Lipids are amphipathic molecules and are one of the main components of biological membranes. Phospholipids are composed of hydrophobic fatty acid chains and hydrophilic headgroups, and along with cholesterol are the primary constituents of eukaryotic cell membranes. In purified forms, lipid/water systems assume a number of liquid-crystalline structures (e.g., lamellae, cubic and hexagonal phases, "rippled" bilayers, etc.), nearly all of which are constructed from a bilayer motif.

Mixtures of long-chain (e.g., 14:0 dimyristoyl phosphatidylcholine (DMPC)) and short-chain (e.g., 6:0 dihexanoyl PC (DHPC)) phospholipids and detergents have emerged as important substrates for nuclear-magnetic-resonance (NMR) studies of biomolecules. These lipid mixtures, also known as bicellar mixtures, exhibit a variety of morphologies depend-

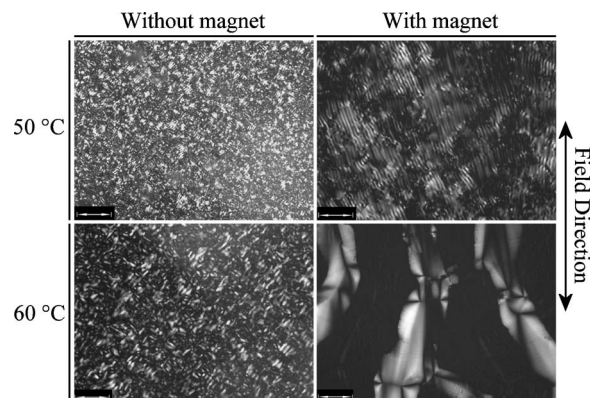


FIG. 3. Micrographs, in the presence and absence of an applied magnetic field, of long-chain DMPC and short-chain DHPC phospholipids ($[\text{DMPC}]:[\text{DHPC}]=3.2$ and $[\text{DMPC}]:[\text{Tm}^{3+}]=75$) in 75 wt% water and two temperatures (50 and 60 °C). From the micrographs, the influence of the magnetic field on the elongated bilayered micelles is obvious. The scale bars represent 0.1 mm.

ing on total lipid concentration, mixing ratios of the short- to long-chain lipids, and temperature. Of particular interest to the NMR community are phases that can align the membrane bilayer in a magnetic field, either spontaneously or on doping with a lanthanide series ion, such as Tm^{3+} .

Recently, a number of studies have shown that the phase behavior of these bicellar mixtures is much more complex than originally thought.^{13–17} Using a combination of polarized optical microscopy¹⁸ (POM) and small-angle neutron scattering (SANS), the phase diagrams of some commonly used nondoped bicellar mixtures have been determined.^{13,16} However, this would not have been possible without the use of POM, as SANS is a costly and time-consuming technique. Comprehensive phase diagrams of magnetic element-doped bicellar mixtures are presently not available, but would be highly sought after since they act as magnetically alignable goniometers for the detailed study of biologically relevant macromolecules. For magnetic ordering of liquid-crystal systems,¹⁹ a typical method is to align the samples off-line and then brought to the microscope for observation.^{20–22} In this case, we wish to study the POM texture of the bicellar system while under a magnetic field to elucidate the conditions of study by NMR.

IV. RESULTS

Figure 3 shows four POM micrographs of a Tm^{3+} -doped bicelle system ($[\text{DMPC}]:[\text{DHPC}]=3.2$, $[\text{DMPC}]:[\text{Tm}^{3+}]=75$, and total lipid concentration of 25 wt%) at 50 and 60 °C, in the presence and absence of a magnetic field. The POM micrographs without the field show a classic fingerprint texture of a cholesteric phase, which from supplementary SANS data, we believe to be a nematic/smectic phase of ribbonlike bilayered micelles.^{13,16} The domains of helical bundles of the micelles at 60 °C are slightly larger than at 50 °C, but in both cases, the domain orientation is random.

With the magnet, we see a dramatic orientation of the micelles at 50 °C. The light and dark bands of the fingerprint texture now run in parallel with the magnetic-field lines. This indicates that the helical axis of the chiral twist runs from left

to right, and most likely places the bilayer normal in this direction as well. In addition, domains are now tens of microns in extent, although the helical pitch (distance between the light and dark bands) is not much different. NMR results predict that the bilayer normal is now parallel to the magnetic field, which would seem to be at odds with the results shown here. At 60 °C, the magnetic field has unexpectedly induced what appears to be a smectic phase. The cholesteric texture is gone, replaced by isotropic domains (in black) bordered by conic defect lines. It is very surprising to observe a magnetically induced, morphological phase transition in this system.

In conclusion these results provide the first visual evidence of the sample conditions of bicellar systems in a magnetic field. Our magnet system demonstrates that it is possible to apply a magnetic field to a specimen under precise environmental conditions, while retaining the important functions of the common benchtop microscope.

ACKNOWLEDGMENTS

The authors wish to acknowledge the helpful advice from their colleague, H. Fritzsche (National Research Council of Canada). T.A.H., M.-P.N. and J.K. acknowledge the financial support received from the Advanced Foods and Materials Network (Networks of Centres of Excellence, Canada).

¹*Electricity and Magnetism in Biology and Medicine*, edited by M. Blank (San Francisco, CA, 1993).

²J. Katsaras, *Phys. Rev. Lett.* **78**, 899 (1997).

³M. Zborowski, G. R. Ostera, L. R. Moore, S. Milliron, J. J. Chalmers, and A. N. Schechter, *Biophys. J.* **84**, 2638 (2003).

⁴J. W. Fassbinder, H. Stanjek, and H. Vali, *Nature (London)* **343**, 161 (1990).

⁵Y. R. Chemla, H. L. Grossman, T. S. Lee, J. Clarke, M. Adamkiewicz, and B. B. Buchanan, *Biophys. J.* **76**, 3323 (1999).

⁶J. R. Dorvee, A. M. Derfus, S. N. Bhatia, and M. J. Sailor, *Nat. Mater.* **3**, 896 (2004).

⁷W. Zheng and G. H. Milburn, *Liq. Cryst.* **27**, 1423 (2000).

⁸J. Gmitrov, C. Ohkubo, and H. Okano, *Bioelectromagnetics (N.Y.)* **23**, 224 (2002).

⁹J. M. Valles, Jr., S. Wasserman, J. M. Denegre, and K. L. Mowry, *Rev. Sci. Instrum.* **71**, 3108 (2000).

¹⁰E. M. Williams, *IEEE Trans. Magn.* **MAG-18**, 1086 (1982).

¹¹R. Oldenbourg and W. C. Phillips, *Rev. Sci. Instrum.* **57**, 2362 (1986).

¹²O. Cugat, P. Hansson, and J. M. D. Coey, *IEEE Trans. Magn.* **30**, 4602 (1994).

¹³T. A. Harroun, M. Koslowsky, M. P. Nieh, C. F. de Lannoy, V. A. Raghunathan, and J. Katsaras, *Langmuir* **21**, 5356 (2005).

¹⁴L. van Dam, G. Karlsson, and K. Edwards, *Biochim. Biophys. Acta* **1664**, 241 (2004).

¹⁵M. -P. Nieh, V. A. Raghunathan, S. R. Kline, T. A. Harroun, C. Y. Huang, J. Pencer, and J. Katsaras, *Langmuir* **21**, 6656 (2005).

¹⁶M. P. Nieh, V. A. Raghunathan, C. J. Glinka, T. A. Harroun, G. Pabst, and J. Katsaras, *Langmuir* **20**, 7893 (2004).

¹⁷M. P. Nieh, C. J. Glinka, S. Krueger, R. S. Prosser, and J. Katsaras, *Langmuir* **17**, 2629 (2001).

¹⁸POM has the ability of differentiating between isotropic and anisotropic materials. Anisotropic materials possess optical properties that vary with the crystallographic axes of the sample, splitting the incident, plane-polarized light into two individual polarized wave components that are in mutually perpendicular planes. Since their velocities are different (i.e., different refractive indices), they become out of phase and are recombined in the analyzer, a second polarizer aligned 90° to the initial polarizer, to yield a characteristic interference pattern.

¹⁹C. Viney, *Polym. Eng. Sci.* **26**, 1021 (1986).

²⁰H. Goto, K. Akagi, and K. Itoh, *Synth. Met.* **117**, 91 (2001).

²¹Y. Oishi, T. Suzuki, H. Awano, and K. Yonetake, *IEEE Trans. Appl. Supercond.* **14**, 1604 (2004).

²²D. H. Van Winkle, A. Chatterjee, R. Link, and R. L. Rill, *Phys. Rev. E* **55**, 4354 (1997).